This article was downloaded by: [Renmin University of China]
On: 13 October 2013, At: 11:07
Publisher: Taylor & Francis
Informa Ltd Registered in England and Wales Registered Number: 1072954 Registered office: Mortimer House, 37-41 Mortimer Street, London W1T 3JH, UK

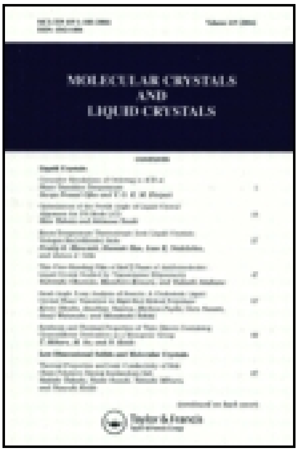

Molecular Crystals and Liquid Crystals
Publication details, including instructions for authors and subscription information:
http://www.tandfonline.com/loi/gmcl20

Optical Microscopic Observation of Morphology in Liquid Crystal/Polymer Composites and Their Electro-Optical Properties

Satoshi Niiyama [a] & Hirotsugu Kikuchi [b]
[a] Research Center , Asahi Glass Co. Ltd. , Kanagawa , Japan
[b] Institute for Materials Chemistry and Engineering , Kyushu University , Fukuoka , Japan

Published online: 09 Jul 2013.

To cite this article: Satoshi Niiyama & Hirotsugu Kikuchi (2013) Optical Microscopic Observation of Morphology in Liquid Crystal/Polymer Composites and Their Electro-Optical Properties, Molecular Crystals and Liquid Crystals, 577:1, 1-14, DOI: 10.1080/15421406.2013.778116

To link to this article: http://dx.doi.org/10.1080/15421406.2013.778116

PLEASE SCROLL DOWN FOR ARTICLE

Taylor & Francis makes every effort to ensure the accuracy of all the information (the “Content”) contained in the publications on our platform. However, Taylor & Francis, our agents, and our licensors make no representations or warranties whatsoever as to the accuracy, completeness, or suitability for any purpose of the Content. Any opinions and views expressed in this publication are the opinions and views of the authors, and are not the views of or endorsed by Taylor & Francis. The accuracy of the Content should not be relied upon and should be independently verified with primary sources of information. Taylor and Francis shall not be liable for any losses, actions, claims, proceedings, demands, costs, expenses, damages, and other liabilities whatsoever or howsoever caused arising directly or indirectly in connection with, in relation to or arising out of the use of the Content.

This article may be used for research, teaching, and private study purposes. Any substantial or systematic reproduction, redistribution, reselling, loan, sub-licensing, systematic supply, or distribution in any form to anyone is expressly forbidden. Terms & Conditions of access and use can be found at http://www.tandfonline.com/page/terms-and-conditions

Mol. Cryst. Liq. Cryst., Vol. 577: pp. 1–14, 2013
Copyright © Taylor & Francis Group, LLC
ISSN: 1542-1406 print/1563-5287 online
DOI: 10.1080/15421406.2013.778116

Optical Microscopic Observation of Morphology in Liquid Crystal/Polymer Composites and Their Electro-Optical Properties

SATOSHI NIIYAMA[1,*] AND HIROTSUGU KIKUCHI[2]

[1]Research Center, Asahi Glass Co. Ltd., Kanagawa, Japan
[2]Institute for Materials Chemistry and Engineering, Kyushu University, Fukuoka, Japan

We have discovered that bicyclohexyl is suitable for extracting liquid crystals from liquid crystal/polymer composites consisting of a continuous phase of nematic liquid crystal and a three-dimensional polymer network. It was confirmed in optical microscopic observation for the morphology of composites that a polymer structure, observed after extraction of liquid crystals from composites by bicyclohexyl, accorded well with the structure observed by a non-destructive method at a higher temperature than the nematic–isotropic transition point of the liquid crystal. The relationship between the polymer structure in the composite which was evaluated by the non-destructive method and the condition of phase separation induced by photo-polymerization was closely investigated from an aspect of a phase diagram and the speed of phase separation controlled by the intensity of irradiation by UV light. The electro-optical characteristics of the liquid crystal/polymer composite cells were found to be strongly affected by the polymer structure, especially the pore size of the three-dimensional network, which was especially sensitive to the intensity of UV light.

Keywords Electro-optical characteristics; liquid crystal/polymer composite; morphology; optical microscopy

1. Introduction

The study of electro-optical characteristics of composite materials comprising liquid crystals and polymers was started by Churchill et al. [1] in the late 1960s as an application of an emulsified cholesteric liquid crystal/polymer binder system to a color display device by applying voltage. Those devices showed high driving voltages and low contrast ratios of the display image with the same result for an application of a sole cholesteric liquid crystal to a display device by Haas et al. [2] because the dielectric anisotropy of available liquid crystal material was small in those days.

As to nematic liquid crystals, Hilsum has discovered an electro-optical effect showing transparency scattering of incident light by index-matching on the application of voltage in a system with liquid crystals and dispersed inorganic micro-particles in it [3]. As to composite material comprising nematic liquid crystals and polymers, Kajiyama et al. [4]

---

[*] Address correspondence to Satoshi Niiyama, Research Center, Asahi Glass Co. Ltd., 1150 Hazawa-cho, Kanagawa-ku, Yokohama, Kanagawa 221-8755, Japan. Tel.: +81-45-374-7416; Fax: +81-45-374-8873. E-mail: satoshi-niiyama@agc.com

first proposed such a composite, which was obtained by evaporating the solvent from a homogeneous solution with liquid crystals and dissolved polymers in a common solvent, and suggested a bi-continuous phase separation of them. Craighead et al. [5] has reported an electro-optical effect of a device using a composite obtained by impregnating liquid crystals into porous polymer film.

For a more practical device using the composite, Fergason [6] has reported a composite structure in which multiple micro-droplets consisting of nematic liquid crystals were dispersed into a polymer matrix by the same emulsion method used for an early composite having cholesteric liquid crystals. The device using a composite composed of liquid crystals having positive dielectric anisotropy and polymers having the same refractive index (n_p) as an ordinary refractive index (n_o) of liquid crystals became transparent when liquid crystal molecules in micro-droplets were aligned parallel to the direction of incident light by applying a voltage to the composite because the refractive index of micro-droplets became almost the same as n_p. The device became opaque to incident light in an electric field in the off state by index-mismatching between polymer matrix and micro-droplets, in which the average directions of liquid crystal molecules did not match the direction of incident light in accordance with the shape of the droplets because the liquid crystal molecules in the droplets were aligned parallel to the interface between the droplets and the polymers.

The emulsion method requires production processes that contain a coating of a solution on a substrate with an electrode, evaporation of the solvent and lamination of a counter substrate, and a bendable film substrate suitable for the process. Doane et al. [7] have solved this issue by proposition of a new production method using no solvent for liquid crystal/polymer composites. The method in which a liquid crystal is phase-separated during polymerization of a low molecular weight curable compound from an isotropic homogeneous solution dissolving liquid crystals into the compound was called Polymerization-Induced Phase Separation (PIPS) and the composite obtained by this method was called Polymer Dispersed Liquid Crystal (PDLC). Vaz et al. [8] have reported composites obtained by photo-polymerization-induced phase separation in a poly-en/poly-thiol system in succession to an early study for thermal-polymerization-induced phase separation in an epoxy prepolymer (P-A) system.

Gunjima et al. have proposed composites obtained by the photo-polymerization-induced phase separation in a radical chain photo-polymerization system using an acrylic P-A [9]. Hirai et al. [10] found out that a polymer phase showing a three-dimensional network having a correlation length of several microns was formed in the continuous liquid crystal phase in a composite via spinodal decomposition by high-speed polymerization-induced phase separation, different from the thermal-polymerization system. Arai et al. have also reported continuous phase-type composites having a polymer network [11]. The continuous phase-type composites showed a higher efficiency of light scattering not only because of index-mismatching between liquid crystal droplets and polymer matrix but also because index-mismatching among adjacent liquid crystal domains was available [12]. Besides, such a composite showed a lower driving voltage because a smaller area of interface between the liquid crystal domain and polymer network led to a smaller fraction of liquid crystal molecules of which alignments were fixed at the interface with the polymer phase. Kunigita et al. have proposed a projection display that combines projection optics with dot-matrix display panels using continuous phase-type composites driven at 10 Volts root mean square (Vrms) or less by thin-film transistors (TFT) [13]. Niiyama et al. [14] have investigated hysteresis on electro-optical characteristics and the response time on a gray scale of a device using composites displaying a moving image.

Studies on the relationship between phase structure and the condition of PIPS by direct observation have been limited, although the formation process from the theoretical aspect of the phase-separated structure for continuous phase-type composites has been precisely investigated by Nwabunma et al. [15], Kyu and Chiu [16], and Nakazawa et al. [17]. The relationship between phase structure and electro-optical characteristics has been reported by Whitehead and Gill [18] in a poly-en/poly-thiol system and by Li et al. in an acrylic P-A system, although the phase structure was observed by means of SEM in both studies [19, 20]. Non-destructive observations by confocal fluorescent microscopy have been reported by Amundson et al. [21] and Tahara et al. [22]; however, comparisons between the phase structure and PIPS condition were limited in both studies because there were several issues such as addition of a fluorescent dye into the composite and limited resolution of the observed images. Besides, the dependence of the liquid crystal content and polymerization condition on a droplet size of a PDLC-type composite in a single acrylic monomer system has been investigated by Ohta et al. [23] based on two-dimensional observation of a phase structure using confocal fluorescent microscopy; however, the electro-optical characteristics were not directly related to the phase structure.

Direct observation of a cell for electro-optical measurement by a non-destructive method is certainly required for investigation of the relationship between the phase structure of a composite and the electro-optical characteristics. In this study, transmission optical microscopy of a cell at a higher temperature than the nematic–isotropic transition temperature of a liquid crystal was carefully examined as a perfectly non-destructive observation method in comparison with observed images before and after extraction of liquid crystals from the composite. For this purpose, a suitable extractant, which could prevent the polymer phase from deforming during the extraction process, was investigated in the former half of this paper.

Effects of phase separation conditions such as liquid crystal content, polymerization temperature, or UV light intensity on the morphologies and those electro-optical characteristics were closely investigated in the latter half of this paper regarding liquid crystal/polymer composites with driving voltages of 10 Vrms or less having a bicontinuous phase of liquid crystal and polymer which were obtained by the photo-polymerization-induced phase separation.

2. Experimental

2.1. Preparation of Liquid Crystal/Polymer Composite

Figure 1 shows the liquid crystal material, P-A, and photo-initiator used in this study. A nematic liquid crystal mixture was used for the liquid crystal (LC) material, and P-A was prepared as a homogeneous mixture with composition shown in Table 1, which shows one oligomer having two acryloyloxy groups and two monomers having one acryloyloxy group. Urethane acrylate was used as a reactive oligomer, which was synthesized in the

Table 1. Composition of prepolymer mixture (wt%)

Oligomer	Monomer A	Monomer B
51.2	12.2	36.6

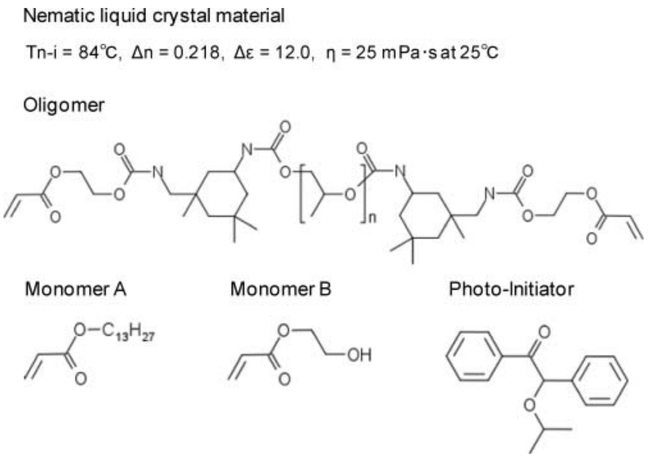

Figure 1. Physical properties of liquid crystal material and chemical structures of prepolymer and photo-initiator.

presence of a tin catalyst from 2 mol of 2-hydroxyethylacrylate and 1 mol of an isocyanate-terminated urethane oligomer synthesized in the presence of the same catalyst from 2 mol of isophorone diisocyanate and 1 mol of poly(propylene glycol) having a number average molecular weight of 1000. Monomer A was a dehydrated compound from acrylic acid and a mixed branched isomer of monohydroxy alcohol, the carbon number of which was 13 (tridecanol [mixed branched isomer], Tokyo Kasei Co. Ltd.), and 2-hydroxyethylacrylate was used for Monomer B. An uncured pre-mixture (M-A) was prepared as a homogeneous solution in which benzoin isopropyl ether (BIPE) as a photo-initiator of 3 wt% was added to the above P-A, and P-A was completely dissolved into liquid crystals in a predetermined amount by heating.

A glass cell used for evaluation of electro-optical characteristics was prepared as follows. A pair of glass substrates on which transparent electrodes made of indium tin oxide (ITO) were formed was laminated facing each electrode, the distance between those substrates due to resin bead spacers and sealed by epoxy resin in a peripheral portion of the substrate was 13 μm. The M-A given above was injected into the cell after the it was heated to be a homogeneous isotropic solution. P-A in M-A was polymerized by BIPE during irradiation of UV light on both sides of the cell from a HgXe lamp having a main wavelength of 365 nm after keeping the temperature of M-A homogeneous isotropic in a thermostatic chamber, and a liquid crystal/polymer composite was obtained from M-A by the photo-polymerization-induced phase separation.

2.2. *Observation of Phase Structure*

The phase structure of the liquid crystal/polymer composite by the cell was observed in a non-destructive method (Observation A) using a transmission bright field optical microscope (BH-2, Olympus Co. Ltd.) while heating the cell at a predetermined temperature with a thermal stage (FP82HT, Mettler-Toledo Inc.).

Polymer film of 1-mm thickness was prepared by photo-polymerization of P-A with BIPE of 3 wt% during irradiation with the same UV light of 20 mW/cm^2 at 25°C for 40 sec. To select a suitable solvent for extraction of liquid crystals from the composite cell, damage

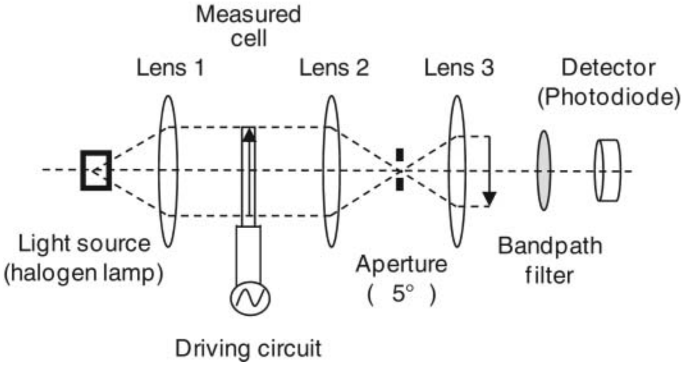

Figure 2. Schematic representation of the measurement system for electro-optical characteristics of liquid crystal/polymer composite cells using the Schlieren optical system.

to the polymer phase by a solvent was evaluated by the measurement of weight change of the film 10 and 60 min after immersion in each solvent at 25°C. Liquid crystals were extracted from the composite by the selected solvent via the cutting plane of glass substrate and composite in the cell during immersion at 40°C for 60 min. The polymer structure was observed (Observation B) in the same way by transmission optical microscope after evaporation of the solvent at 266 Pa at 80°C for 60 min.

2.3. Electro-optical Characteristics

The electro-optical characteristics of the liquid crystal/polymer composite cell were evaluated at 40°C in a thermostatic chamber by Schlieren optics having a collection angle of 5°, as shown in Fig. 2. The intensity of the transmitted light through the cell was measured by a photodiode with a bandpass filter having a center wavelength of 540 nm and a half-band width of 20 nm using a halogen lamp as an incident light source. Transmittance was measured by applying alternative voltage of 30 Hz in rectangular waveform between transparent electrodes of a cell having a voltage increase rate of 10 Vrms/min using a functional generator (3114A, Hewlett-Packard Co.) and high-speed amplifier (4010, NF Corp.) as the power supply for driving.

3. Results and Discussion

3.1. Phase Diagram of Liquid Crystal and Prepolymer

Evaluation of a phase diagram is very important in the formation of a phase separation structure, and the optimum polymerization temperature is determined based on it in PIPS. Figure 3 shows a phase separation temperature at which M-A becomes turbid by segregation of liquid crystals from M-A under decreasing temperature, and a phase mixing temperature at which M-A turns into a homogeneous state by dissolution of the liquid crystal in M-A under increasing temperature. The intensity of the transmitted light from He–Ne laser as a light source through M-A in a clear bottle was measured by a photodiode on stirring M-A with a magnetic stirrer installed in a thermobath, which was controlled at a temperature increase/decrease rate of 1°C/min. The segregation temperature (T_s) and dissolution temperature (T_d) indicate respectively the decreasing temperature at which

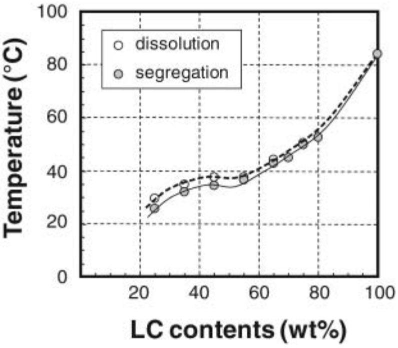

Figure 3. Phase diagram of M-A (LC/P-A/BIPE). Solid line shows segregation temperature on cooling and broken line shows dissolution temperature on heating.

M-A starts to become turbid and the increasing temperature at which the whole of M-A becomes transparent.

A liquid–liquid phase separation phenomenon was observed in liquid crystal content of not more than 50 wt% since the temperature difference between T_s and T_d was about 4°C. On the other hand, a segregation phenomenon of liquid crystal, that is a liquid–liquid crystal phase separation phenomenon, was observed in higher liquid crystal content since the temperature difference became smaller. To obtain a uniform structure of the liquid crystal/polymer composite, the polymerizing temperature of M-A is required to be higher than T_s to prevent phase separation by temperature. Besides, a composite comprising a larger amount of phase-separated liquid crystal might be obtained by PIPS at as low temperature as possible because it is assumed that the phase separation line between segregation and dissolution shifts to a higher temperature region in the phase diagram after polymerization of the P-A is finished [10, 23].

3.2. Observation of Liquid Crystal/Polymer Composite by Transmission Optical Microscope

Glass-sandwiched cells filled with the composites of various liquid crystal contents were prepared by PIPS of M-A comprising liquid crystals of 25/35/45/55/65/75 wt% during UV irradiation of 10 mW/cm^2 from each side of cell at $T_s + 0.5$°C at decreasing temperature. Figure 4 shows transmittance optical microscope images of the obtained cells under crossed polarizers. The cells of composites made up of liquid crystals of more than 45 wt% were seen as opaque by uniformly scattering incident light. The cells consisting of liquid crystals

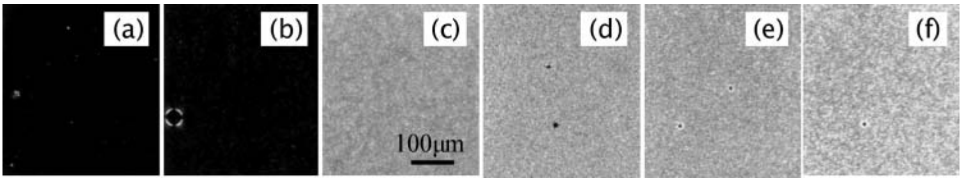

Figure 4. Optical microscopic images under crossed polarizers of composites after photo-polymerization-induced phase separation from M-A. Content of liquid crystal in each M-A is as follows: (a) 25 wt%, (b) 35 wt%, (c) 45 wt%, (d) 55 wt%, (e) 65 wt%, (f) 75 wt%.

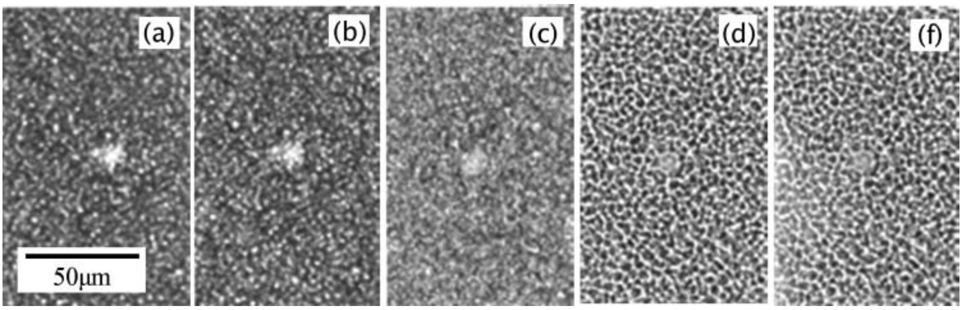

Figure 5. Optical microscope images of composite after photo-polymerization induced-phase separation from a mixture comprising LC of 75 wt% and P-A at several temperatures. The temperature for observation is controlled by hot stage at (a): 40°C, (b): 60°C, (c): 80°C, (d): 90°C, (e): 100°C.

of 65 wt% and 75 wt% showed strong light scattering in particular. On the other hand, the cells of composites comprising liquid crystal of not more than 35 wt% were transparent and no phase-separated structure was observed. It was difficult to precisely observe the phase-separated structure because the incident light from the light source for observation was optically modulated by birefringence of the phase-separated liquid crystal phase, although slight differences in the texture in accordance with liquid crystal content were observed in cells of composites having liquid crystals of more than 45 wt%.

3.3. Observation by Transmission Optical Microscope in Isotropic Phase (Observation Method A)

Figure 5 shows transmission optical microscope images of the cell with liquid crystals of 75 wt% observed at each temperature according to "Observation A." The glass substrate of the cell facing an objective lens was optically polished down to about 150 μm to accommodate the distance between the lens and the cell to a focal depth of the objective lens. A three-dimensional network structure in the phase-separated polymer phase was observed at a higher temperature than 90°C which is more than the nematic–isotropic transition point (Tn-i) of the liquid crystal though subtle changes of the images were also observed at not more than 80°C. It was found that the texture of the phase-separated structure was clearly observed by the difference of indices between the isotropic liquid crystal phase and the polymer phase even in transmission optical microscopic observation because birefringence of the liquid crystals disappeared at a higher temperature than Tn-i. Resin spacers having a diameter of 13 μm controlling the distance between the electrodes of the cell are shown near the center of the images in Fig. 5.

3.4. Transmission Optical Microscopic Observation After Extraction of Liquid Crystal (Observation Method B)

The validity of observation method A was investigated by comparing it with "Observation B." Table 2 shows the solubility for liquid crystals with regard to various solvents and degrees of swelling of polymer film obtained by polymerization of P-A for 10 min and 60 min after immersion in each solvent to select a suitable solvent for extraction of liquid crystal via the cutting plane of composite cell. An extractant, which has superior solubility for liquid crystals and shows a lower degree of swelling of the polymer phase, is required

Table 2. Solubility of several solvents for LC and swelling property of polymerized P-A in those solvents

Solvent	Solubility for liquid crystal	Weight increase of polymerized P-A in solvent (wt%) 10 min	60 min
Dichloromethane	Good	250	Break
THF	Good	165	236
Chloroethanol	Good	136	204
1,4-dioxane	Good	129	201
Aceton	Good	134	177
Toluene	Good	128	166
Ethyl acetate	Good	129	178
Benzyl alcohol	Good	117	148
Cyclohexane	Marginal	106	114
Cyclooctane	Marginal	104	108
Bicyclohexyl	Marginal	101	103
Ethanol	Poor	—	—
Isopropanol	Poor	—	—
n-hexane	Poor	102	106

for preventing the polymer phase from deforming during extraction of liquid crystals. It was found that solvent having a cyclo-aliphatic structure showed a lower degree of swelling of the polymer phase, although heating to around 40°C was required to dissolve liquid crystal because the solubility was limited. Most solvents with good solubility for liquid crystals tended to swell the polymer phase. On the other hand, solvents showing lower degrees of swelling had lower solubility for liquid crystals, as shown in Table 2. Bicyclohexyl was selected as extractant for the extraction of liquid crystals by observation method B.

The solvent in which liquid crystal was easily dissolved at 25°C was rated as "good," the one in which liquid crystal was dissolved with heat at around 40°C was rated as "marginal," and the solvent in which liquid crystal hardly dissolved at 40°C was rated as "poor." Weight increase of polymer film after being immersed in the solvents at 25°C for 10 and for 60 min are shown in Table 2.

Figure 6 shows a transmission optical microscope image of a cell having liquid crystals of 75 wt% after extracting one part. The three-dimensional network structure of the polymer phase was clearly observed in Area B, where the liquid crystal was extracted, although the precise texture was not observed in Area A, where the liquid crystal still existed because the incident light from the light source for observation was optically modulated by birefringence of the liquid crystal phase.

Figure 7 shows transmission optical microscope images of cells with liquid crystals of more than 45 wt% after extraction of liquid crystal by bicyclohexyl. The morphologies of the polymer network were observed in all cells of composites showing the liquid crystal phase in the transmission optical microscope images shown in Fig. 4. The pore size of the polymer network in the composite became larger according to the liquid crystal content and pores having the diameter of several micrometers were observed in composites with

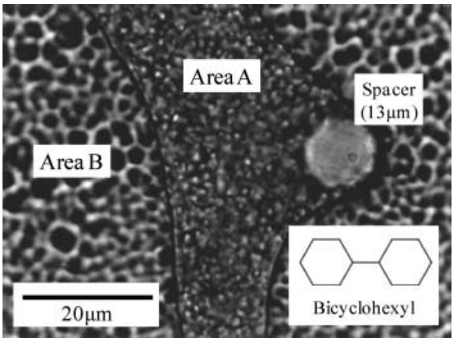

Figure 6. Optical microscopic image of composite consisting of LC of 75 wt% after partially extracting LC from composite by bicyclohexyl as extractant. Area A shows composite phase with LC and polymer phase, and area B shows polymer phase without LC.

liquid crystals of 75 wt%. It is concluded that observation method A is a simpler and valid observation method because almost the same polymer network pore sizes were observed in both images obtained after extraction of liquid crystals shown in Fig. 7(d) and the image obtained at 90°C without extraction by observation method A shown in Fig. 7(e), which is a transmission optical microscopic observation of the composite having liquid crystals of 75 wt%.

3.5. *Morphologies of Polymer Network for Composite Cells and Those Electro-Optical Characteristics*

Figure 8 shows the electro-optical characteristics of composite cells made up of liquid crystals of more than 45 wt%, as shown in Fig. 7. Optical transmittance was measured by increasing the applied voltage using the Schlieren optical system shown in Fig. 2. The cells of a composite comprising liquid crystals of 45 wt% showed a small change in transmittance with applied voltage. It is suggested that the smaller pore size of the polymer network shown in Fig. 7 induced a lower mobility of liquid crystal molecules in the liquid crystal domain held in the network. Threshold voltages at which the light-scattering state

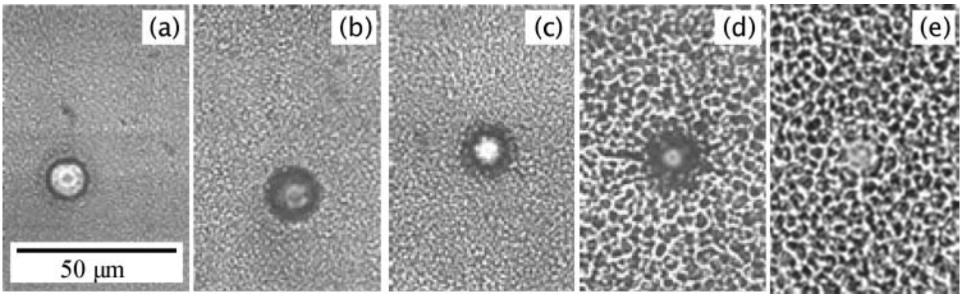

Figure 7. Optical microscopic images of polymer phase in composites after extraction of LC by bicyclohexyl as extractant. Contents of LC in those composites are (a) 45 wt%, (b) 55 wt%, (c) 65 wt%, and (d) 75 wt%. Polymer phase with LC of 75 wt% is shown in comparative microscope image (e) observed at 90°C (>Tn-i of LC).

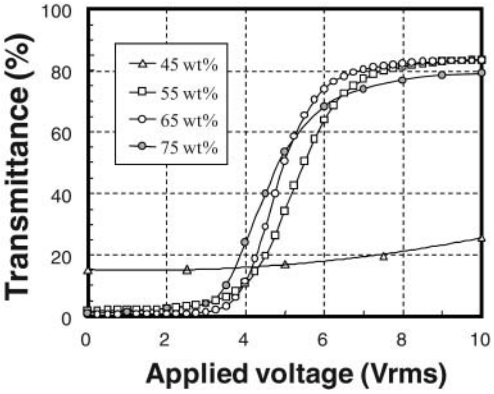

Figure 8. Electro-optical characteristics of composites having LC of 45/55/65/75 wt%. Transmittance was measured at 40°C through a bandpath filter of 540 nm ($\Delta\lambda = 20$ nm) in front of the detector on increasing applied voltage at 10 Vrms/min.

started to change into a transparent state for the cells of composites comprising liquid crystals of more than 55 wt% tended to decrease according to the content of liquid crystals. A change in the threshold voltage was unexpectedly small, although the pore size of the polymer network strongly depended on the content of liquid crystals. On the other hand, the cells of a composite with the liquid crystals of 65 wt% showed the steepest change in transmittance versus the applied voltage (Δ Transmittance/Δ Applied voltage). It is considered that a uniform phase-separated structure having almost the same pore size as the liquid crystal domain can be obtained by phase separation from a specific position in the phase diagram shown in Fig. 3, because the size of the liquid crystal domain is assumed to affect the threshold voltage.

To investigate the effect of temperature in the phase diagram on the morphology of polymer network, the cells of composites comprising liquid crystals of 65 wt% were prepared by PIPS at various temperatures. Fig. 9 shows the morphologies observed by observation method A of the cells, which were obtained by photo-polymerization with UV light intensity of 20 mW/cm^2 at the segregation temperature of liquid crystals (T_s) + ΔT. Uniform morphologies were observed in all cells obtained at temperatures higher

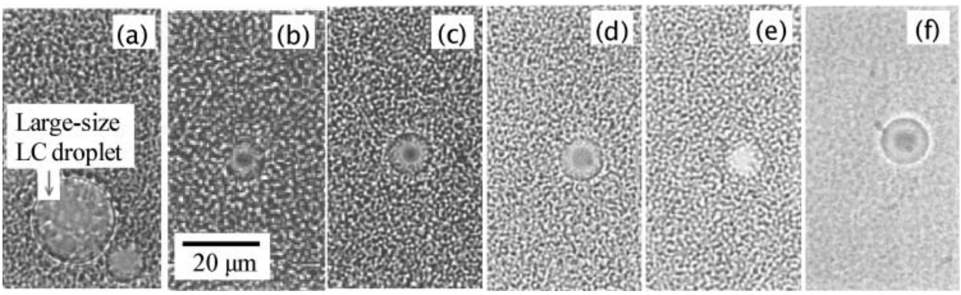

Figure 9. Optical microscopic images of composites phase separated at the segregation temperature $T_s + \Delta T$ in the phase diagram: (a) $\Delta T = -0.2$°C, (b) +0.5°C, (c) +2.0°C, (d) +4.0°C, (e) +8.0°C, (f) +16°C. All images were observed at 86°C (>Tn-i of LC).

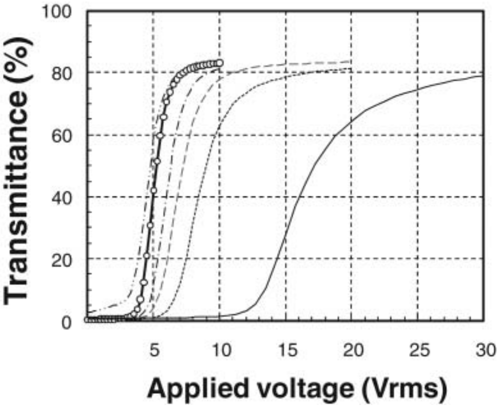

Figure 10. Electro-optical characteristics of composites phase-separated at the segregation temperature (T_s) +ΔT in the phase diagram, (–●●–): ΔT = −0.2°C, (–○–): +0.5°C, (–●–): +2.0°C, (– – –): +4.0°C, (- - - - - -): +8.0°C, (——): +16.0°C.

than T_s, as shown in Figs. 9(b)–(f). Macro-segregation of the liquid crystal was observed in cells obtained by phase separation at lower temperatures than T_s, as shown in Fig. 9(a). The polymer network tended to have a thick branch and a smaller pore size according to the increased temperature difference between T_s and the polymerization temperature. The contrast ratio of the observed image for a cell is obtained at $T_s + 16°\mathrm{C}$, as shown in Fig. 9(f). It is suggested that the difference in indices between the isotropic liquid crystal phase and the polymer phase became smaller because the liquid crystal molecules might be dissolved in the polymer phase in case of a large temperature difference between T_s and the polymerization temperature.

Figure 10 shows the electro-optical characteristics for the cells of composites with liquid crystals of 65 wt% obtained by phase separation at various temperatures, as shown in Fig. 9. The cells of a composite obtained at a lower temperature than T_s showed a little weak intensity of light scattering in an electric field in the off state and higher transmittance at a low applied voltage because of macro-segregation of the liquid crystal, as shown in Fig. 9(a). The cells of composites obtained at higher temperatures than T_s showed higher threshold voltages according to an increase in temperature difference between T_s and the polymerization temperature. It is considered that the threshold voltage increased because the size of the liquid crystal domain decreased according to a decrease in the pore size of the polymer network, as shown in Fig. 9. It is also assumed that the composite obtained at the polymerization temperature of $T_s + 16°\mathrm{C}$ showed an even higher threshold voltage because interaction on liquid crystal molecules increased at the interface of the phase-separated polymer phase in which a part of the liquid crystal molecules remained.

The cells of composites comprising liquid crystals of 65 wt% were prepared by the photo-polymerization-induced phase separation using UV light irradiation of various intensities at the polymerization temperature of $T_s + 0.5°\mathrm{C}$, which gave the steepest threshold voltage, as shown in Fig. 10. Fig. 11 shows the morphologies of the polymer phase in the cells observed by observation method A. It is considered that the speed of the photo-polymerization-induced phase separation is controlled by the intensity of UV light irradiation. In accordance with the increase of the intensity of UV light irradiation, the pore size of the polymer network significantly increased and its distribution was also enlarged. A nearly two-dimensional structure of the polymer phase due to segregation of the liquid

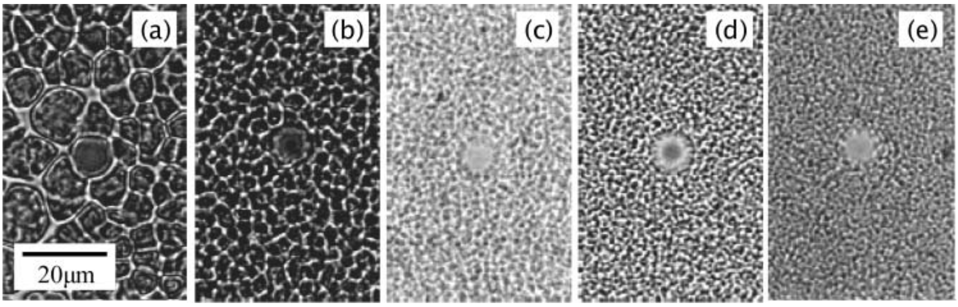

Figure 11. Optical microscopic images of composites photo-polymerized by UV light irradiation of various intensities: (a) 0.2 mW/cm^2, (b) 1.0 mW/cm^2, (c) 6.0 mW/cm^2, (d) 20 mW/cm^2, (e) 28 mW/cm^2. All images were observed at 86°C (>Tn-i of LC).

crystal was observed in the cell of a composite obtained by UV light irradiation of 0.2 mW/cm^2, as shown in Fig. 11(a). It is assumed that part of the P-A remained in the liquid crystal phase because the area of polymer network observed in Fig. 11(a) was even smaller than the content of the P-A in M-A.

Figure 12 shows the electro-optical characteristics for the cells of composites comprising liquid crystals of 65 wt% obtained by the photo-polymerization-induced phase separation by UV light irradiation of various intensities, as shown in Fig. 11. The threshold voltage for the cell significantly decreased according to a decrease in the intensity of UV light irradiation. Light scattering in an electric field in the off state was very weak in the cell of a composite obtained by UV light irradiation of not more than 1.0 mW/cm^2. It is suggested that a larger liquid crystal domain, in accordance with the pore size of the polymer network, gave both lower scattering efficiency for visible light by a scattering cross section and a smaller number of liquid crystal domains in the direction of incident light.

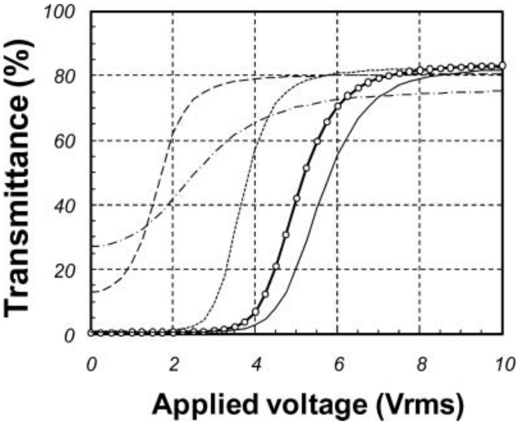

Figure 12. Electro-optical characteristics of composites photo-polymerized by UV light irradiation of various intensities: (–●–): 0.2 mW/cm^2, (– – –): 1.0 mW/cm^2, (------): 6.0 mW/cm^2, (–○–): 20 mW/cm^2, (——): 28 mW/cm^2.

4. Conclusion

It was found that bicyclohexyl is a suitable extractant for extraction of liquid crystals from a liquid crystal/polymer composite comprising a continuous liquid crystal phase and a three-dimensional polymer network by preventing the polymer phase from swelling with it during the extraction. Network structures of the polymer phase were clearly observed after extraction of the liquid crystal, although it had been difficult to observe a composite structure by an ordinary transmission optical microscope because the incident light from the light source for observation was optically modulated by birefringence of liquid crystal. Perfectly non-destructive observation of the polymer network structure was achieved by optical microscopic observation at a higher temperature than the nematic–isotropic transition point of liquid crystal without its extraction. The image by non-destructive observation accorded well with the morphology observed after extraction of liquid crystal by bicyclohexyl.

Composites having different morphologies of the polymer phase were obtained by the photo-polymerization-induced phase separation from various positions (content of liquid crystal/polymerization temperature) in the phase diagram of a composition having liquid crystals and P-A. The cell with the steepest change in transmittance versus the applied voltage was obtained by a composite with liquid crystals of 65 wt% phase-separated at a slightly higher temperature than the segregation temperature of liquid crystals. The low-intensity of UV light irradiation for photo-polymerization gave a large pore size for the polymer network. It is considered that a large pore size led to weak light scattering in an electric field in the off state and low threshold voltage in electro-optical characteristics.

References

[1] Churchill, D., & Cartmell, J. (1971). US Patent No. 3600060.
[2] Haas, W., Adams, W., & Flannery, J. (1972). US Patent No. 3680950.
[3] Kajiyama, T., Nagata, Y., Maemura, E., & Takayanagi, M. (1979). *Chem. Lett.*, *8*, 679.
[4] Hilsum, C. (1976). UK Patent No. 1442360.
[5] Craighead, H. G., Cheng, J., & Hackwood, S. (1982). *Appl. Phys. Lett.*, *40*, 22.
[6] Fergason, J. L. (1985). *SID 85 Digest*, *16* 68.
[7] Doane, J. W., Vaz, N. A., Wu, B.-G., & Zumer, S. (1986). *Appl. Phys. Lett.*, *48*, 269.
[8] Vaz, N. A., Smith, G. W., & Montgomery, G. P. (1987). *Mol. Cryst. Liq. Cryst.*, *146*, 1.
[9] Gunjima, T., Kumai, H., Tsuchiya, S., & Masuda, K. (1989). US Patent No. 4834509.
[10] Hirai, Y., Niiyama, S., Kumai, H., & Gunjima, T. (1990). *Rep. Res. Lab. Asahi Glass Co.*, *40*, 285.
[11] Arai, Y., Fujisawa, T., Takeuchi, K., Takatsu, H., Adachi, K., Ogawa, H., & Maruyama, K. (1996). European Patent No. 313053.
[12] Kajiyama, T., Miyamoto, A., Kikuchi, H., & Morimura, Y. (1989). *Chem. Lett.*, *18*, 813.
[13] Kunigita, M., Hirai, Y., Ooi, Y., Niiyama, S., Asakawa, T., Masumo, K., Kumai, H., Yuki, M., & Gunjima, T. (1990). *SID 90 Digest*, *9*, 227.
[14] Niiyama, S., Hirai, Y., Ooi, Y., Kunigita, M., Kumai, H., Wakabayashi, T., Iida, S., & Gunjima, T. (1993). *SID 93 Digest*, *11*, 869.
[15] Nwabunma, D., Chiu, H.-W., & Kyu, T. (2000). *J. Chem. Phys.*, *113*, 6429.
[16] Kyu, T., & Chiu, H.-W. (2001). *Polymer*, *42*, 9173.
[17] Nakazawa, H., Fujinami, S., Motoyama, M., Ohta, T., Araki, T., Tanaka, H., Fujisawa, T., Nakada, H., Hayashi, M., & Aizawa, M. (2001). *Comput. Theor. Polym. Sci.*, *11*, 445.
[18] Whitehead, J. B., & Gill, N. L. (2005). *SPIE*, *5741*, 83.
[19] Li, W., Cao, Y., Kashima, M., Kong, L., & Yang, H. (2008). *J. Polym. Sci. B Polym. Phys.*, *46*, 1369.

[20] Li, W., Cao, Y., Kashima, M., Liu, F., Cheng, Z., Yang, Z., Zhu, S., & Yang, H. (2008). *J. Polym. Sci. B Polym. Phys.*, *46*, 2090.

[21] Amundson, K., Blaaderen, A., & Wiltzius, P. (1997). *Phys. Rev. E*, *55*, 1646.

[22] Tahara, S., Niiyama, S., Kumai, H., & Wakabayashi, T. (1998). *SPIE*, *3297*, 44.

[23] Ohta, S., Inasawa, S., & Yamaguchi, Y. (2012). *J. Polym. Sci. B Polym. Phys.*, *50*, 863.